01

# Modeling of surface-volumetric charging of a dielectric irradiated by electrons with energy range from 6 to 30 keV

© V.M. Zykov, D.A. Neyman

Tomsk Polytechnic University,
Tomsk, Russia
e-mail: Neyman@tpu.ru

*Received February 11, 2023*
*Revised April 3, 2023*
*Accepted April 10, 2023*

The physico-mathematical model applied to ground tests for geomagnetic plasma exposure based on the combined consideration of surface and bulk processes of transport and charge accumulation for calculating the kinetics of charging high-resistance dielectrics irradiated by medium-energy monoenergetic electrons (from 6 to 30 keV) is proposed. The model takes into account the contribution to the charging of the dielectric by the trains of longitudinal optical phonons generated by each thermalizing primary electron with energy below the band gap of the dielectric, which supplements the induced conduction current due to the generation of electron-hole pairs. As a result, the current induced by trains of longitudinal optical phonons of the tunnel conductivity through free electron traps is introdused, as well as the current induced in the conduction band due to multiphonon ionization the electron traps by trains of longutudinal optical phonons in the region of existence of electric field. Using the example of the $\alpha$-$Al_2O_3$ (sapphire) dielectric, the results of computer simulation of the internal currents distributions, charges, and electric field in the dielectric with the open surface irradiated by monoenergetic electrons with energies from 6 to 30 keV are presented according with the achievement the quasi-equilibrium in the irradiated part of the dielectric and with switching of the energy of primary electrons during the irradiation process.

**Keywords:** dielectric, surface charging, volumetric charging, surface-volumetric model, secondary electron emission, tunnel current, phonons.

DOI: 10.61011/TP.2023.06.56522.21-23

## Introduction

The relevance of studying the processes of radiative electrostatic charging of dielectrics by medium-energy electrons, corresponding to the low-energy part of geomagnetic plasma electrons, is due to the need to prevent powerful electric discharge processes both on surfaces and in the power cable network of spacecraft (SC) [1]. The upper limit of the spectrum of EM interference caused by electric discharge processes during radiative electrostatic charging of solar cells by geomagnetic plasma electrons in the normal potential gradient mode reaches several GHz [2–7], which indicates that the rise time of the discharge current can be about 1 ns. In this case, the average value of the discharge current flowing through the protective glasses of the photoconverters of solar cells and the back electrode reaches 25 A, and the amplitude value of the discharge current can reach 100 A [1]. Besides, the results of studying the processes of electrostatic charging of dielectrics find application in such areas as electron lithography [8,9], scanning electron spectroscopy and microscopy [10]. The reason for this is the significant difference between the processes of electrons interaction with charged and uncharged dielectric, which is especially evident at energies up to 30 keV.

Currently, information about the electric charges stored in structural dielectrics and internal electric fields is obtained from the results of ground test-bed tests for the effect of geomagnetic plasma, in which the charge effect of geomagnetic plasma is modeled by a flow of monoenergetic electrons with an energy of about 10 keV, where the main informative parameters are the magnitude of the surface electric potential of the dielectric, with respect to the potential of the metal substrate and the potential of the walls of the vacuum chamber (collecting electrode), as well as the density of the current flowing through the metal substrate during charging. However, these parameters are less informative for estimating the internal electric fields of the dielectric, since they weakly depend on the distribution of excess internal charges in the dielectric. Besides, as a rule the process of charging the structural dielectrics with open surface occurs in the presence of electric discharge plasma, in which the negative surface potential of the dielectric is completely or partially neutralized by positive ions from the electric discharge plasma and from the ionized residual atmosphere. Namely under the conditions of neutralization of the surface potential of the dielectric by ions of the electric discharge plasma the dangerous internal charges and electric fields are created, leading both to internal electrical breakdowns of the dielectric with plasma ejection towards vacuum, and to local breakdowns of the dielectric throughout its entire thickness. This mechanism takes place in the case of protective glasses of spacecraft solar cells, which have thickness of about several lengths of the maximum range of primary electrons.

In view of the foregoing, there is a need to create and verify a computer model for charging structural dielectrics with medium-energy electrons, capable of estimating the dynamics of internal distributions of electric charges in dielectrics irradiated by medium-energy electrons, taking into account the electrical state of the dielectric surface and specific test-bed conditions of irradiation, including presence of electric discharge plasma. Such computer model can be used to recalculate the test results obtained at the test-bed to full-scale space conditions.

Most of the papers related to the dielectrics charging processes are based on the description, mainly, of bulk processes of charge transport and accumulation. These works can include the so-called double layer formation model and its modifications [11–14], in which the main sources of fields are charges formed as a result of secondary electron emission (SEE) electrons exit and injection by means of primary electrons with energy from 1 to 30 keV.

In the paper [15] it was shown that additional consideration of the surface charge, i.e. charge localized on the open surface of the dielectric, as well as the conductive environment leads to qualitatively different results in the charging kinetics. In particular, during long-term irradiation a strong inversion of the subsurface field can be observed, this field is formed due to bulk electrons (major carriers) captured by surface traps.

In this paper we propose a model that takes into account the charging by electrons of a thin surface layer of the dielectric containing a high concentration of charge traps associated with structural surface defects, and the charging of the dielectric surface is possible both from the side of the bulk of the dielectric and from the outer side, which is in contact, for example, with electrical discharge plasma. Besides, the model takes into account the multiphonon mechanism of electron tunneling through deep traps and the multiphonon mechanism of electron release from deep traps due to trains of longitudinal optical phonons (LO-phonons) generated by each thermalizing primary electron of geomagnetic plasma decelerated down to the energy equal and below the band gap width of the dielectric.

The results analysis [16,17] shows that primary electrons during their thermalization are responsible for the high rate of generation of LO-phonon trains. Also note that the generation rate of phonons exceeds the rate of their absorption, thereby leading to their accumulation. The presence of a high concentration of LO-phonons as a result of irradiation with primary electrons contributes to increase in the frequency factor of the tunneling transition of the electron, due to multiphonon process, from the occupied trap to the free one. Besides, in actual dielectrics there is increased concentration of deep traps in the near-surface region, among which there are also deeper traps than in the bulk [18] due to defects in the near-surface region. This mechanism generates the additional tunnel current of electrons, which, in the presence of increase in the concentration of deep traps towards the surface, is enhanced towards the surface of the dielectric and is the additional source of negative charging of surface.

Within the framework of the model, as applied to the crystalline dielectric $\alpha$-$Al_2O_3$ (sapphire), the time dependences of the potential (flying energy) of the open surface of the dielectric are determined. The main regularities of changes in the surface density of charge, concentrations of the bulk excess charge of electrons and holes, as well as the electric field depending on the coordinate (through the thickness of the dielectric) and time are established. Examples are given of modeling the process of dielectric charging in a variable environment that simulates the spacecraft entry into the Earth's radiation belt or the consequences of a solar flare. The influence of the process of charging the defective surface of the dielectric by internal currents initiated by external electron irradiation were evaluated. Estimates were obtained for changes in the spatial distributions of the electric field, as well as for electrons and holes in traps in a two-stage process of establishment of charge quasi-equilibrium, first in the part of the dielectric irradiated by primary electrons and then in the part not irradiated by primary electrons. The calculation algorithm of the model makes it possible, if necessary, to calculate the charging under conditions of contact of the dielectric surface with the electric discharge plasma or with the ionized residual atmosphere.

## 1. Physical concept of the model

The model was made within the framework of a one-dimensional approximation by analogy with the diagram shown in Fig. 1 as a further development of the model [15]. In the experiment this geometry takes place when the beam width significantly exceeds the penetration depth of primary

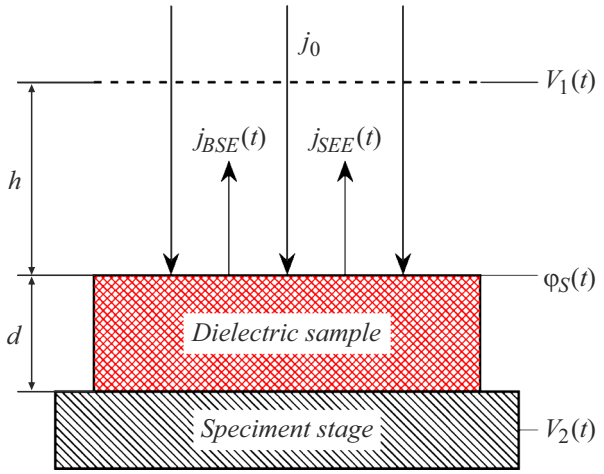


**Figure 1.** Schematic representation of experimental setup (test=bed, microscope) corresponding to the present model. Here $V_1(t)$ and $V_2(t)$ — are the potentials of the collecting electrode and the adjacent metal substrate, respectively, $\varphi_S(t)$ — the potential of the open surface of the dielectric, $j_{SEE}(t)$ — SEE current density, $j_{BSE}(t)$ — current density of backscattered electrons.

electrons into the dielectric bulk, which in most cases also corresponds to scanning electron microscopes (SEM) in the scanning mode or in the defocused beam mode.

The charging model $\alpha$-$Al_2O_3$ is considered, in which a sample with thickness of $d$ has a back electrode on the unirradiated surface, where $d$ can vary from a value of about the range of the primary electron to several millimeters. The open surface is irradiated with medium-energy electrons and is separated from the conducting environment (for example, from a screening metal collecting electrode or from the boundary corresponding to the Debye radius of the plasma) by a vacuum gap $h$ thick. Depending on the test conditions, the valu $h$ can take a wide range of values, starting from $h \sim 1$ cm (SEM conditions) [10] or $h \sim 1$ m (test-bed Prognoz 2), or limited by the Debye radius of plasma in geostationary orbit $h \sim 100$ m [1]. The collecting electrode and the back electrode can be at the potentials $V_1(t)$ and $V_2(t)$, respectively.

### 1.1. Surface and near-surface model

It is assumed that actual sample has a thin damaged surface layer (TDSL) containing a high concentration of electron traps and a transient near-surface layer (Fig. 2) from a high concentration of electron traps on the surface to a lower concentration of electron traps in the bulk of the dielectric.

TDSL can exchange electrons with the bulk of the dielectric through currents flowing in the near-surface layer of the dielectric, such as induced conduction currents, as well as diffusion and drift currents.

The outer side of the TDSL dielectric is able to retain the charge for a long time, including the charge deposited on it from the side of the vacuum gap, for example, due to the deposition of ions from the residual gas atmosphere or ions from the surrounding low-temperature electric discharge plasma.

It is assumed that the near-surface region contains at least by an order of magnitude greater number of deep electron traps, which decrease exponentially deep into the dielectric and equalizing with the bulk concentration of traps:

$$N_t(x) = N_{SDT} \exp(-x/X_{TUN}) + N_{DT}, \tag{1}$$

where $N_{SDT}$ — surface concentration of free traps of charge carriers (electrons); $N_{DT}$ — average bulk concentration of deep electron traps; $X_{TUN}$ — parameter characterizing the runoff factor of the near-surface concentration.

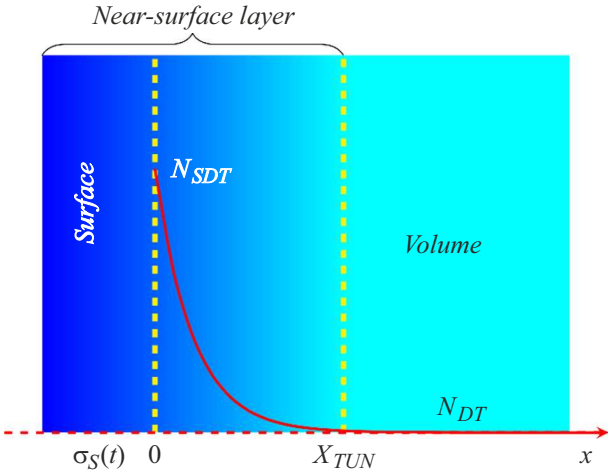


**Figure 2.** Model of dielectric near-surface layer.

### 1.2. Main system of equations

The description of the dielectric charging kinetics, in general terms, is given by a system of equations consisting of the Poisson equation and the continuity equation [19].

It is assumed that the considered dielectric $\alpha$-$Al_2O_3$ (sapphire) has the electron conductivity type [20], while the mobility of holes is neglected. The bulk of the dielectric is considered as a structure containing many traps $N_{DT} \sim 10^{25}\,\mathrm{m}^{-3}$ [21], the main part of which is occupied by deep electron-type traps, the role of which is played by oxygen vacancies ($F+$ and $F$ centers) [20,22,23].

In view of the foregoing, the present model is built in the approximation that all processes are explicitly expressed in terms of charge distribution densities of electrons $\rho^-_{DT}(x,t)$ and holes $\rho^+_{DT}(x,t)$ located in deep traps. Thus, for the Poisson equation we have

$$-\varepsilon_r\varepsilon_0\nabla^2\varphi(x,t) \approx \rho^-_{DT}(x,t) + \rho^+_{DT}(x,t), \tag{2}$$

where $\varphi(x,t)$ — potential of the electric field in the bulk of the dielectric; $\varepsilon_r$ — relative permittivity of dielectric; $\varepsilon_0$ — electrical constant.

Here and below, the reference point $x = 0$ is tied to the surface layer/dielectric interface, and the positive direction is set in the direction of dielectric thickness increasing.

To take into account the influence of the vacuum chamber wall and the back electrode, which are at the potentials $V_1(t)$ and $V_2(t)$, as well as the surface charge density of the surface layer $\sigma_S(t)$, the equation (2) is supplemented with boundary conditions:

$$\varphi(-h,t) = V_1(t), \tag{3}$$

$$\big(\varphi(0,t) - V_1(t)\big)\frac{\varepsilon_0}{h} - \varepsilon_0\varepsilon_r\nabla\varphi(x,t)\big|_{x=0} = \sigma_S(t), \tag{4}$$

$$\varphi(d,t) = V_2(t). \tag{5}$$

The dynamic component of the model is given by the continuity equation, which is represented by a system of charge balance equations, each of system components describes the change in the concentrations of electrons (6) and holes (7) trapped in deep traps, respectively:

$$\frac{\partial\rho^-_{DT}(x,t)}{\partial t} = S_n(x,t) - \frac{\partial j^-_{DIF}(x,t)}{\partial x} - \frac{\partial j^-_{DFT}(x,t)}{\partial x} - \frac{\partial j_{TUN}(x,t)}{\partial x} - \frac{\partial j_{TF}(x,t)}{\partial x} + g^-_{RAD}(x,t) + \frac{\partial\rho_{REC}(x,t)}{\partial t}, \tag{6}$$

$$\frac{\partial \rho_{DT}^{+}(x,t)}{\partial t} = -\frac{\partial j_{SEE}(x,t)}{\partial x} + g_{RAD}^{+}(x,t) - \frac{\partial \rho_{REC}(x,t)}{\partial t}, \quad (7)$$

$$\frac{\partial \sigma_S(t)}{\partial t} = -j_S(t). \quad (8)$$

The right-hand parts of equations in system (6)–(8) are as follows:

$S_n(x,t)$ is the rate of capture of primary-beam electrons by deep traps (determined using the Monte Carlo method); $j_{DIF}^{-}(x,t)$ is the electron diffusion current density; $j_{DFT}^{-}(x,t)$ is the electron drift current density; $j_{SEE}(x,t)$ is the SEE electron current density; $g_{RAD}^{-}(x,t)$ and $g_{RAD}^{+}(x,t)$ correspond to nonpositive and nonnegative values of derivative $-\partial j_{RAD}(x,t)/\partial x$, where $j_{RAD}(x,t)$ is the current density of intrinsic and radiation-induced conduction that is related to the production of electronhole pairs; $j_{TUN}(x,t)$ is the tunnel current density of charge captured by deep traps that is induced by trains of LO phonons, which are produced by each thermalizing electron, in the region of gradient of empty deep traps; $j_{TF}(x,t)$ is the conduction current density due to multiphonon ionization induced by trains of LO phonons, which are produced by each thermalizing electron; and $j_S(x,t)$ is the density of current charging the dielectric surface.

Note that in system (6)–(8) the approximation is made in which the excess radiation-induced charge is considered to be immediately trapped by deep traps. Such approximation takes place due to the high concentration of deep traps in the bulk of the dielectric $N_{DT} \sim 10^{25}\,\mathrm{m}^{-3}$ [21], the probability of being trapped in these traps noticeably exceeds the probability of recombination between free electrons and holes trapped in deep traps $\rho_{DT}^{+}(x,t)$. Further correction occurs due to recombination with near-surface holes, which remained after the release of SEE electrons and were also trapped by deep traps.

The electron part of the distribution $\rho_{RAD}^{-}(x,t)$ is localized mainly near the open surface of the dielectric and participates in processes of recombination with near-surface holes left after the SEE electrons exit. The hole part $\rho_{RAD}^{+}(x,t)$ extends deep into the dielectric and has significantly lower charge densities both in comparison with its electron component $\rho_{RAD}^{-}(x,t)$ and in comparison with the density of electrons $\rho_{DT}^{-}(x,t)$, trapped by deep traps.

The recombination in equations (6) and (7) between electrons entered the conduction band and holes trapped in deep traps is determined by the relation

$$\frac{\partial \rho_{REC}(x,t)}{\partial t} = \frac{k_{REC}}{e_0} W_{PF}(x,t) |\rho_{DT}^{-}(x,t) \rho_{DT}^{+}(x,t)|, \quad (9)$$

where $k_{REC}$ — coefficient responsible for the recombination rate; $e_0$ — elementary charge.

The ionization rate of deep traps $W_{PF}(x,t)$ in expression (9) depending on the electric field and temperature as applied to electrons is calculated by the Poole-Frenkel formula multiplied by a function that takes into account the concentration gradient of free traps in the near-surface region of the dielectric:

$$W_{PF}(x,t) = \left(1 - \left(1 - \frac{N_{DT}}{N_{SDT}}\right) \exp\left(-\frac{x}{X_{TUN}}\right)\right) \times \exp\left(\frac{\beta_F \sqrt{|F(x,t)|}}{k_B T}\right), \quad (10)$$

where $\beta_F = (e_0^3/\pi\varepsilon_r\varepsilon_0)^{1/2}$ — Frenkel parameter; $F(x,t)$ — electric field; $k_B$ — Boltzmann constant; $T$ — temperature.

The rate of change of the surface charge is taken into account by means of relation (8), and the current density $j_S(t)$ is the sum of the currents flowing to the surface both from the side of the bulk of dielectric and from the side of the vacuum gap, for example, currents of low-energy ions from the gas environment (plasma). If the electric field in the vacuum gap is inverted, i.e., $F_V(t) < 0$, then the current $j_S(t)$ also includes electrons returned to the surface. In particular, for the case of high vacuum and flying energy $E_L(t) > E_{k2}$, where $E_{k2}$ is the second crossover energy, one can use the relation

$$j_S(t) = j_{RAD}(0,t) + j_{DIF}^{-}(0,t) + j_{DFT}^{-}(0,t) + j_{TUN}(0,t) + j_{TF}(0,t). \quad (11)$$

At the point of zero field, the electron drift stops, which leads to local accumulation of charges in adjacent regions and the appearance of large concentration gradients. Thus, the microrelief of the electrons distribution in the conduction band $W_{PF}(x,t)\rho_{DT}(x,t)$, created near the specific points, requires small values of the computational grid spacing for its consideration in the calculation by the finite difference method. This, in turn, due to the accumulation of errors, makes it difficult to calculate the processes at large times responsible for the shift of the second critical electron energy for the SEE electron exit.

In view of the foregoing, the calculation at large times, comparable with the time for the achievement by electron flying energy $E_L(t)$ of the second critical energy $E_{k2}$ for the charged dielectric, is possible only by averaging the current distributions over intervals exceeding the characteristic length of the microrelief of these distributions near specific points and in the local region of the strong electric field.

### 1.3. Electric field

Solving the system (2) –(5) and taking into account the relation $F(x,t) = -\mathrm{grad}\varphi(x,t)$, we obtain a formula describing the distribution of the resulting electric field inside the dielectric, i.e. field, which takes into account the distribution of both the volumetric charge inside the dielectric and the charge that is concentrated in the surface layer of the dielectric:

$$F(x,t) \approx F(0,t) + \frac{1}{\varepsilon_0\varepsilon_r} \int_0^x \rho(\xi,t)\,d\xi, \quad (12)$$

where $\rho(x,t) = \rho^{-}_{DT}(x,t) + \rho^{+}_{DT}(x,t)$ is the total density of the excess (nonequilibrium) charge on deep traps in the bulk of the dielectric.

In relation (12) the internal subsurface field of the open side of the dielectric $F(0,t)$ is given by a formula that includes the parameters of the environment geometry $h$ and $d$ , as well as the function of the influence of the external source on the field distribution inside the dielectric in the form of surface charge density $\sigma_S(t)$ on the surface and the potential values of the conducting environment $V_1(t)$ and $V_2(t)$:

$$F(0,t) = \frac{1}{d+\varepsilon_r h}\left(\sigma_S(t)\frac{h}{\varepsilon_0} - \frac{1}{\varepsilon_0\varepsilon_r} \times \int_0^d (d-\xi)\rho(\xi,t)d\xi + V_1(t) - V_2(t)\right). \quad (13)$$

### 1.4. Current of secondary electron emission

The current density of SEE electrons, which depends on the electric field in the near-surface region of the dielectric, in the simplest case can be approximated by the expression [15]:

$$j_{SEE}(x,t) = j_0\delta_{SEE}(t)\exp\left(-\frac{1}{s_0}\int_0^x \exp\big(-\beta_E F(\xi,t)\big)d\xi\right), \quad (14)$$

where $j_0$ — current density of the primary electron beam; $\delta_{SEE}(t)$ — SEE electron yield factor, which is a function of the subsurface electric field $F(0,t)$; $\beta_E$ — parameter of electron current weakening by electric field. The dependence of the SEE electron yield on time in expression (14) is calculated by the formula [24]:

$$\delta_{SEE}(t) = A\frac{E_L(t)}{E_i}\alpha^{-1}(t)\big[1-\exp(-\alpha(t))\big],$$

$$\alpha(t) = \frac{R(t)}{s(t)}, \quad s(t) = s_0\exp(\beta_E F(0,t)), \quad (15)$$

where $A$ — selected parameter (probability of exit from depth $s(t)$), $E_i$ — ionization energy of a neutral dielectric atom, $s_0$ — average depth of SEE electrons yield in the absence of the electric field, $R(t)$ — maximum penetration length of primary electrons with flying energy $E_L(t)$ into the bulk of the dielectric.

### 1.5. Diffusion and drift currents

The density of diffusion and drift currents of charge carriers (electrons) is determined by the expressions

$$j^{-}_{DIF}(x,t) = -D_n^{\text{eff}}\frac{\partial}{\partial x}\big(W_{PF}(x,t)\rho^{-}_{DT}(x,t)\big), \quad (16)$$

$$j^{-}_{DFT}(x,t) = -\mu_n^{\text{eff}}W_{PF}(x,t)\rho^{-}_{DT}(x,t)F(x,t), \quad (17)$$

where $D_n^{\text{eff}} = D_n P_n$ — diffusion coefficient of free electrons, taking into account the probability $P_n$ of the electron entering the conduction band with subsequent trapping by deep trap, $\mu_n^{\text{eff}} = D_n^{\text{eff}} e_0/k_B T$ – the mobility of free electrons, expressed by the diffusion coefficient in accordance with the Einstein formula.

### 1.6. Currents of intrinsic and radiation-induced conduction

The classical expression for the current density of intrinsic and radiation-induced conduction, provided that the electric field is relatively small $F(x,t) \le 10^6\ \text{V}\cdot\text{cm}^{-1}$ (as applied to $\alpha$-$Al_2O_3$), is described by Ohm's law

$$j_{RAD}(x,t) = \big(\sigma_D + \sigma_{RIC}(x,t)\big)F(x,t), \quad (18)$$

where $\sigma_D$ — intrinsic conductivity, and radiation-induced conductivity is determined according to the Rose-Fowler formula [25], $\sigma_{RIC}(x,t) = k_{RIC}\dot{D}(x,t)^{\Delta}$, in which $\dot{D}(x,t)$ — dose rate distribution; $k_{RIC}$ — coefficient of radiation-induced conductivity; $\Delta$ —parameter that depends on the type of material and varies from 0.5 to 1 ($\alpha$-$Al_2O_3$).

Accounting for trains of LO-phonons generated by each primary thermalizing electron with an energy below the dielectric band gap (for $\alpha$-$Al_2O_3$ below 10 eV), leads to the presence of additional components of induced conductivity. In particular, it becomes necessary to take into account the tunneling current $j_{TUN}(x,t)$ of electrons in free deep traps in the concentration gradient region of these traps, as well as the current $j_{TF}(x,t)$ associated with multiphonon ionization due to trains of optical phonons.

Thus, the total current density of intrinsic and radiation-induced conduction within the framework of the model takes the form

$$j^{\Sigma}_{RAD}(x,t) = j_{RAD}(x,t) + j_{TUN}(x,t) + j_{TF}(x,t). \quad (19)$$

#### 1.6.1. Tunneling current through deep traps due to LO-phonon trains

In the available publications [17,20,26–38] relating the calculation of the tunneling current of electrons maintained by phonons through traps in the dielectric, the situation is not considered in which the decelerating electrons of the primary beam with energy below 10 eV actively participate in the generation of phonons.

Thus, in the proposed model, the following key features of electron tunneling in the dielectric between deep traps under conditions of irradiation with low-intensity medium-energy electron beam (6–30 keV) are distinguished:

• Each primary electron of the beam after completion of the processes of generation of electron-hole pairs, but before thermalization, having the energy from value slightly exceeding the phonon generation threshold to values of about 10 eV, intensely generates the train of oscillations of optical and acoustic phonons over a time of 200 fs [16].

• Each trap electron, being in a deep potential trap, together with its held dielectric atoms, participates in phonon oscillations of these atoms, periodically acquiring sufficiently high kinetic energy (up to several eV), which is maily determined by the train of LO phonons produced by each thermalizing electron of the beam. As a result, the trap electron periodically rises to the edge of the potential well of the trap, getting the opportunity to make a tunnel transition or to enter the conduction band.

• If the dielectric has the structure of a crystal, then the LO-phonon vibrations of this crystal atoms and, consequently, the kinetic energy of the trapped electron associated with them are strictly oriented with respect to the crystallographic direction so that the trapped electron can leave the given trap only in 2 opposite directions, oriented to the nearest free traps of the crystal structure, for example, oxygen vacancies.

• If an electron trapped in the deep trap is in excited state due to interaction with the train of LO-phonons, then it will most likely leave the trap in the direction from which the average distance to the nearest free trap will be less. The average interval between the generation of LO-phonon trains, thermalized in the crystal by electrons:

$$\Delta t_{PE} = \frac{e_0}{j_{PE}(0,t)S_k}, \tag{20}$$

where $j_{PE}(0,t)$ is the current density of the primary electron beam injected into the dielectric; $S_k$ — crystal area, which is irradiated by the transverse beam.

Let the number of trap electrons participating in the shift towards the surface by the value of the average distance $\langle l_{TUN}\rangle = \sqrt[3]{N_t(x)}$ between traps is equal to $\rho_{DT}^{-}(x,t)W(x,t)/e_0$, where $W(x)$ — probability of the trap electron participation in the shift to the surface at distance $\langle l_{TUN}\rangle$ during the action of the next LO-phonon train. Then the effective velocity of the trap electrons through the traps is equal to

$$v_{te}(x) = \frac{1}{\Delta t_{PE}\sqrt[3]{N_t(x)}}. \tag{21}$$

The probability $W(x)$ can be represented as the product of the coefficient of proportionality $k_{TUN}$ and the concentration gradient of free electron traps

$$W(x) \approx k_{TUN}|\mathrm{grad}N_t(x)| = k_{TUN}\frac{N_{SDT}}{X_{TUN}}\exp\left(-\frac{x}{X_{TUN}}\right). \tag{22}$$

For the tunneling current density at depth $x$, we obtain the expression

$$j_{TUN}(x,t) = v_{te}(x)\rho_{DT}^{-}(x,t)W(x) \tag{23}$$

or explicitly

$$j_{TUN}(x,t) = k_{TUN}\frac{N_{SDT}}{X_{TUN}}\, j_{PE}(0,t)S_k N_t(x)^{-1/3} \times \rho_{DT}^{-}(x,t)\exp\left(-\frac{x}{X_{TUN}}\right). \tag{24}$$

Assuming that the probability of the trap electron tunneling to the neighboring trap depends on the distance $\langle l_{TUN}\rangle$ to it as [26]:

$$\propto \frac{1}{\langle l_{TUN}\rangle^2}\exp\left(-2\langle l_{TUN}\rangle\frac{\sqrt{2m^*E_T}}{\hbar}\right), \tag{25}$$

where $m^*$, $E_T$ and $\hbar$ — are the effective electron mass, trap depth, and Planck's constant, respectively.

Taking into account the above for the tunneling current density in deep traps, we have

$$j_{TUN}(x,t) = k_{TUN}P(x,L_{ph})\frac{N_{SDT}}{X_{TUN}}\, j_{PE}(0,t)S_k N_t(x)^{1/3} \times \rho_{DT}^{-}(x,t)\exp\left(-\frac{x}{X_{TUN}}\right), \tag{26}$$

where $P(x,L_{ph})$ is the quantity that considers the fraction of all electrons in the primary beam that contribute to the generation of LO-phonon trains at the point $x$, depending on the average attenuation length of optical phonons $L_{ph}$.

Thus, by introducing an additional parameter $L_{ph}$, which characterizes the average decay length of optical phonons, it becomes possible to take into account both short-range and long-range orders in the dielectric, going, respectively, from the amorphous phase to the crystalline one.

### 1.6.2. Current due to multiphonon ionization stimulated by LO-phonon trains

The presence of zero field point deep in the dielectric ($x \approx 10^{-6}$ m) leads to increase in the electron concentration $n_{DT}^{-}(x,t)$ in this region. A similar situation arises in the near-surface region at a depth of 1 nm [15]. Accounting for the current $j_{TF}(x,t)$, which depends on the electric field in the near-surface region of the dielectric, contributes, along with other currents, to additional suppression of the growth of inhomogeneities in the distribution of electrons in traps, which, among other things, has a positive effect on the computational characteristics of the model.

Assuming the rate of generation of free electrons by LO phonon trains proportional to the current density of primary electrons, we have

$$W_{tr}(x,t) \propto j_{PE}(x,t)\frac{S_k}{e_0}. \tag{27}$$

The average drift lengths of the released electrons in opposite directions, orthogonal to the open surface of the dielectric, are determined by the expressions

$$\lambda_{RE}\big(F(x,t)\big) = \lambda_{E0}\exp\big(+\beta_E F(x,t)\big), \tag{28}$$

$$\lambda_{TE}\big(F(x,t)\big) = \lambda_{E0}\exp\big(-\beta_E F(x,t)\big), \tag{29}$$

where $\lambda_{E0}$ is the average electron drift length in the absence of the electric field $F(x,t)$, and $\lambda_{TE}\big(F(x,t)\big)$ and $\lambda_{RE}\big(F(x,t)\big)$ are the mean electron drift lengths in the forward direction, i.e., to the back electrode, and in the opposite directions in the presence of the electric field, respectively.

### 1.7. Thickness of dielectric $d \gg R_{\max}(E_L)$

If we assume that the concentrations of free deep traps in the near-surface region are sufficiently high $N_{SDT} \sim 10^{26}\,\mathrm{m}^{-3}$, then we can assume that the electrons released due to the LO-phonon train, after movement to distance $\lambda_E\big(F(x,t)\big)$ are trapped by free traps and do not recombine with near-surface holes. In this case, the average velocity of electrons in traps (taking into account the exit to the conduction band) is given by the expressions

$$v_{RE}(x,t) = \lambda_{RE}\big(F(x,t)\big)W_{tr}(x,t), \tag{30}$$

$$v_{TE}(x,t) = \lambda_{TE}\big(F(x,t)\big)W_{tr}(x,t). \tag{31}$$

Then the current density in deep traps (taking into account the drift in the conduction band) can be expressed as the algebraic sum of two components of the current densities:

$$j_{TF}(x,t) = j_{RE}(x,t) - j_{TE}(x,t) = \frac{1}{2}\rho_{DT}^{-}(x,t)[v_{RE}(x,t) - v_{TE}(x,t)], \tag{32}$$

where the coefficient 1/2 is related to equal proportion of electrons moving in the forward and reverse directions when entering the conduction band.

Taking into account the expressions for the rate of electron generation due to LO-phonon trains (27), as well as the transport average velocities (30) and (31), the above expression can be represented as

$$j_{TF}(x,t) = k_{TF}P(x,L_{ph})\frac{S_k}{2e_0}\,j_{PE}(x,t)\rho_{DT}^{-}(x,t) \times \big[\lambda_{RE}\big(F(x,t)\big) - \lambda_{TE}\big(F(x,t)\big)\big], \tag{33}$$

where $k_{TF}$ — coefficient that can be selected on the basis of experimental data.

## 2. Experimental results

Below there are the results of modeling the kinetics of charging the high-resistance dielectrics using the example of widespread oxide $\alpha$-$Al_2O_3$ (sapphire) (see Table), corresponding to various initial conditions $j_0$, $E_0$, at zero boundary conditions $V_1(t) = V_2(t) = 0\,\mathrm{V}$ and $h = 1\,\mathrm{m}$ (thereby simulating the laboratory conditions of charging in conducting environment, which correspond to space conditions with a Debye radius equal and over 1 m [1]).

Main parameters $\alpha$-$Al_2O_3$ (sapphire)

| Parameter | Values | Units |
|---|---|---|
| $\varepsilon_r$ | 10 | |
| $\mu_n$ | $4 \cdot 10^{-4}$ [21] | $\mathrm{m}^2/(\mathrm{V{\cdot}s})$ |
| $\mu_p$ | $2 \cdot 10^{-7}$ [21] | $\mathrm{m}^2/(\mathrm{V{\cdot}s})$ |
| $v_{th}$ | $10^5$ [21] | m/s |
| $E_g$ | 9 [21] | eV |
| $\rho$ | 3.98 | $\mathrm{kg/m}^3$ |
| $k_{RIC}$ | $4.6 \cdot 10^{-16}$ [39] | $\mathrm{S{\cdot}s^{\Delta}/(m{\cdot}rad^{\Delta})}$ |
| $N_{DT}$ | $10^{25}$ | $\mathrm{m}^{-3}$ |
| $N_{SDT}$ | $10^{26}$ | $\mathrm{m}^{-3}$ |

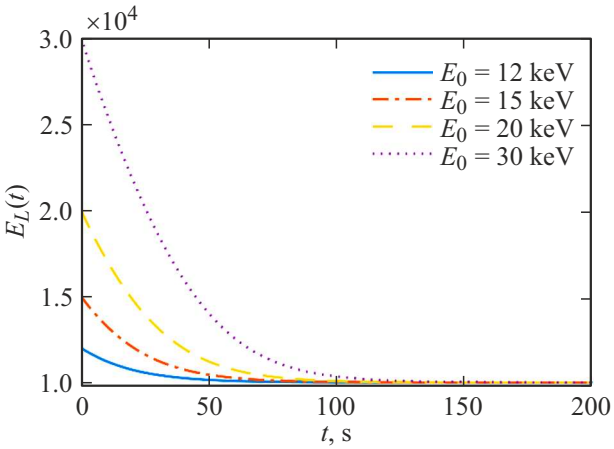


**Figure 3.** Incoming energy of primary electrons vs. irradiation time at different initial energies $E_0$. Here $j_0 = 10^{-4}\,\mathrm{A/m}^2$, $d = 1\,\mathrm{mm}$, $h = 1\,\mathrm{m}$.

Fly-in energy of primary electrons Fig. 3 at initial energies $E_0$ in the range from 12 to 30 keV and current density $j_0 = 10^{-4}\,\mathrm{A{\cdot}m^{-2}}$ reaches quasi-equilibrium in the irradiation time interval from 50 to 100 s at dielectric thickness $d = 1\,\mathrm{mm}$. The current density $j_{TUN}(0,t)$ in the near-surface region of the dielectric, due to the presence of a large concentration gradient of free traps, contributes to a strong influx of electrons from the bulk to the surface of the dielectric, which is illustrated by the time dependence of the total current $j_S(t)$, charging surface (Fig. 4), most of which is formed by the currents $j_{TUN}(0,t)$, $j_{TF}(0,t)$ and $j_{RIC}(0,t)$. As a result, there is an inversion of the subsurface field of the dielectric $F(0,t) < 0$ (Fig. 5) occurs, which leads to the formation of a zero field point near the open surface at a depth of about 1 nm.

It can be seen from Fig. 6 that the maximum fraction of the surface charge in relation to the charge stored in the bilk at $N_{SDT}/N_{DT} = 10$ reaches 8% at energies of primary electrons $E_0$ close to $E_{k2}$. The exit of SEE electrons, along with the injection of primary electrons, leads to the formation of two main distribution centers of holes $n_{DT}^{+}(x,t)$ and electrons $n_{DT}^{-}(x,t)$ trapped in deep traps. The first of which is located in the near-surface region, the second — in the depth of the irradiated region of the dielectric. The change in the dependences of these distributions for the energy $E_0 = 15\,\mathrm{keV}$ is illustrated in Figs 7 and 8.

Analyzing the data corresponding to the initial energy $E_0 = 15\,\mathrm{keV}$, it can be seen that quasi-equilibrium in the charge distribution curves corresponds to the times of equilibrium for the current $j_S(t)$ charging the dielectric surface.

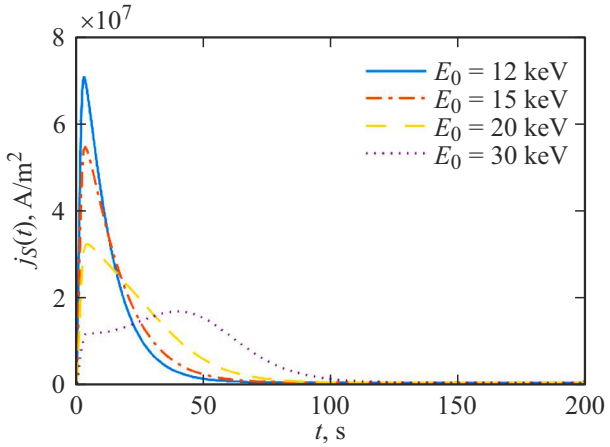


**Figure 4.** Total current density, charging dielectric surface vs. irradiation time at different initial energies of primary electrons $E_0$. Here $j_0 = 10^{-4}$ A/m$^2$, $d = 1$ mm, $h = 1$ m.

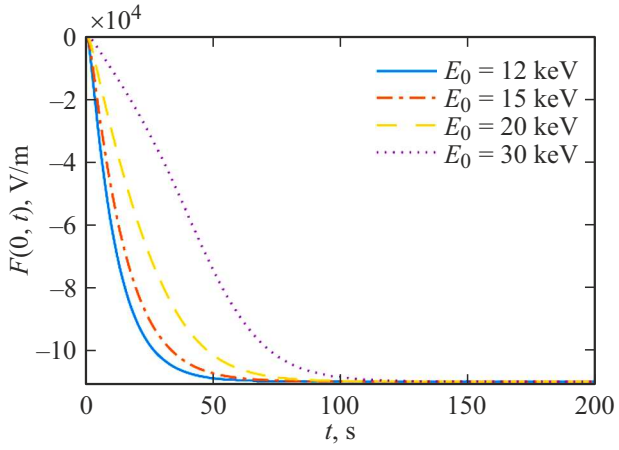


**Figure 5.** Subsurface field vs. irradiation time at different initial energies $E_0$. Here $j_0 = 10^{-4}$ A/m$^2$, $d = 1$ mm, $h = 1$ m.

The presence of the first electric field maximum $F_{\max 1}$ ($x \approx 1.5 \cdot 10^{-8}$ m (Fig. 9)) leads to enhanced ionization of deep electron traps, as a result the Poole-Frenkel effect, followed by the recombination of released electrons with holes $n^+_{DT}(x,t)$, which is manifested by the depletion of the distributions of both electrons and holes in deep traps in this region (Fig. 7 and 8).

Holes generated as a result of radiation-induced conduction, due to recombination lead to gradual neutralization of the central part ($x \approx 3.5 \cdot 10^{-7}$ m) of the distribution $n^-_{DT}(x,t)$ of electrons trapped in deep traps. It is also reflected in the electric field distribution in Fig. 9. Rate of holes generation in the depth of the dielectric can exceed the rate of their recombination, which in our case leads to increase in the holes concentration of holes in the depth of the dielectric($x \approx 3.5 \cdot 10^{-6}$ m (see insert Fig. 7)), forming another positive charge center near the second maximum of the electric field $F_{\max 2}$.

### 2.1. Thickness of dielectric $d$ is close to $R_{\max}(E_L)$

Actual issues relate to the charging of dielectrics, the actual thickness of which reaches $\sim 100\,\mu$m (for example, light-conducting protective coatings of solar cells of spacecrafts).

When the thickness of the dielectrics is comparable to the maximum range of primary electrons, a feature appears in the charging kinetics associated with the two-stage process of establishment of charge quasi-equilibrium.

In particular, for the initial energy $E_0 = 15$ keV on the graph of the total current of electrons charging the surface $j_S(t)$ (Fig. 10), flowing from the bulk of the dielectric, the two-stage process is observed: the first stage of a rapid change in currents at relatively small times $\sim 50$ s, the second stage is a long-term negative charging of the surface.

In contrast to similar processes at thicknesses $d \gg R_{\max}(E_L)$, the surface potential (fly-in energy $E_L(t)$)

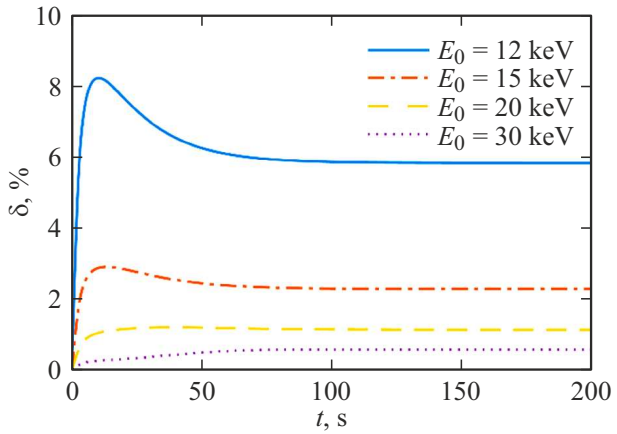


**Figure 6.** Fraction of charge stored on surface traps with relation to total charge in bulk of dielectric $E_0$. Here $j_0 = 10^{-4}$ A/m$^2$, $d = 1$ mm, $h = 1$ m.

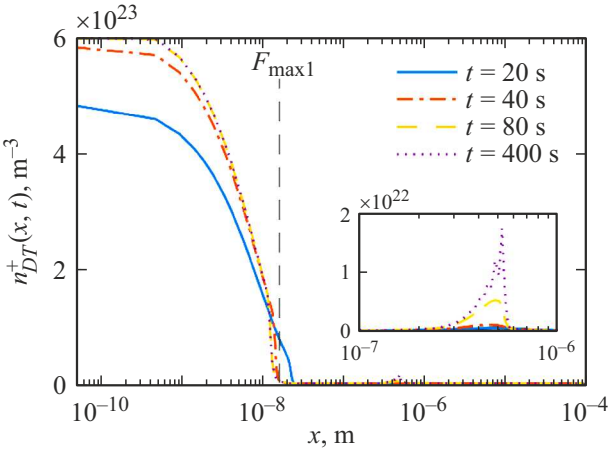


**Figure 7.** Distribution of holes left after release of SEE, trapped by deep traps at initial energy $E_0 = 15$ keV, corresponding to different times. Here $F_{\max 1}$ —is the coordinate of the first electric field maximum, $j_0 = 10^{-4}$ A/m$^2$, $d = 1$ mm, $h = 1$ m.

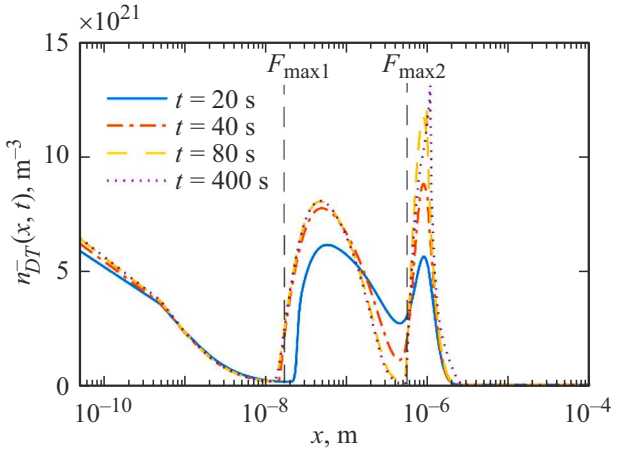


**Figure 8.** Distribution of electrons trapped by deep traps at initial energy $E_0 = 15$ keV, corresponding to different times. Here $F_{max\,1}$ and $F_{max\,2}$ are the coordinates of the first and second maximums of the electric field, respectively, $j_0 = 10^{-4}$ A/m$^2$, $d = 1$ mm, $h = 1$ m.

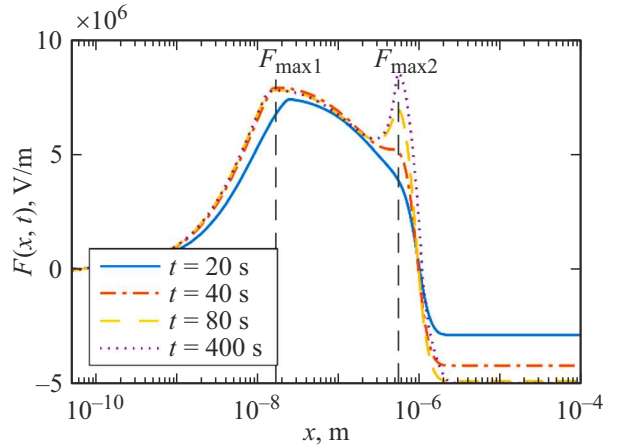


**Figure 9.** Distribution of electric field at initial energy $E_0 = 15$ keV, corresponding to different times. Here $F_{max\,1}$ and $F_{max\,2}$ are the coordinates of the first and second maximums of the electric field, respectively, $j_0 = 10^{-4}$ A/m$^2$, $d = 1$ mm, $h = 1$ m.

does not reach the equilibrium state during the time to reach quasi-equilibrium by surface current $j_S(t)$. In particular, it can be seen from Figs 11 and 12 that the onset of the quasi-equilibrium state in the irradiated region (depth up to $2 \cdot 10^{-6}$ m) does not correspond to the time of the first stage completion on the dependences of currents $j_S(t)$ Fig. 10.

Further charging of the dielectric leads to increase in the distribution of electrons trapped by deep traps in the vicinity of the second point of the zero field ($x \approx 10^{-6}$ m) on the side of positive values of the electric field. In the region of the negative electric field (Fig. 11), due to its large magnitude, there is a strong outflow of electrons towards the back electrode due to the deep traps ionization with subsequent drift in the electric field.

## 2.2. Variable radiation environment

When the spacecraft enters the Earth's radiation belt or as a result of the solar flare the initial conditions for dielectric charging may change. This situation often occurs in natural conditions, but is not yet reproduced in standard test methods for radiative electrostatic charging.

The present model allows simulating such a situation as switching the initial energy $E_0$ and/or the initial current density $j_0$, which gives more opportunities to verify the model and to bring the result closer to the natural environment.

One of the advantages of switching the initial conditions (by the example of switching the initial energy $E_0$) is the possibility to realize the case corresponding to the flying energy $E_L(t)$ less than $E_{k2}$ for charged dielectrics. In particular, Fig. 13 shows that after changing the initial energy $E_0$ from 20 to 12 keV, the flying energy decreases to $E_L \approx 6$ keV. Further, the incoming energy $E_L(t)$ changes to

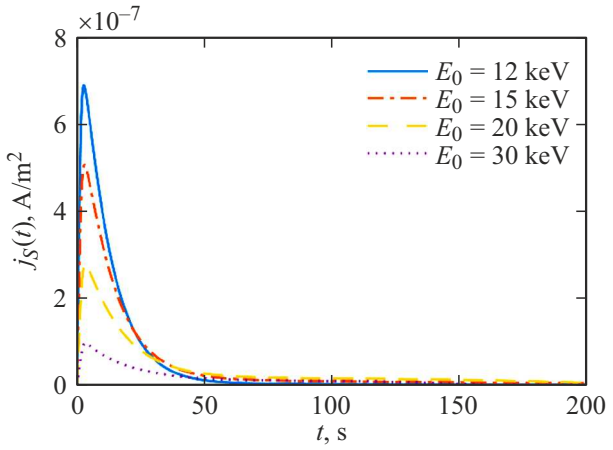


**Figure 10.** Total current density, charging dielectric surface vs. irradiation time at different initial energies of primary electrons $E_0$. Here $j_0 = 10^{-4}$ A/m$^2$, $d = 100\,\mu$m, $h = 1$ m.

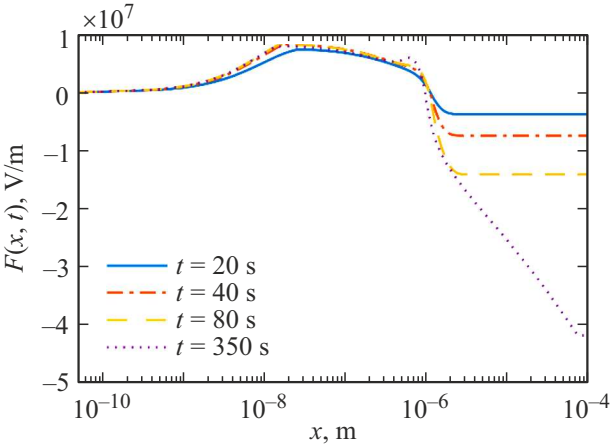


**Figure 11.** Distribution of electric field at initial energy of primary electrons $E_0 = 15$ keV, corresponding to different times. Here $j_0 = 10^{-4}$ A/m$^2$, $d = 100\,\mu$m, $h = 1$ m.

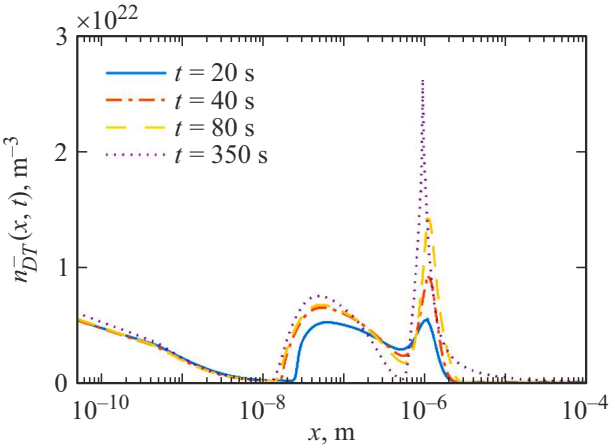


**Figure 12.** Distribution of electrons trapped by deep traps at initial energy $E_0 = 15$ keV, corresponding to different times. Here $j_0 = 10^{-4}$ A/m$^2$, $d = 100\,\mu$m, $h = 1$ m.

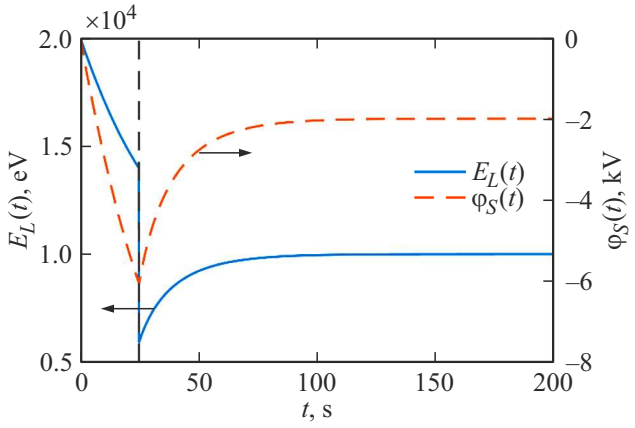


**Figure 13.** Fly-in energy of primary electrons vs. time in mode of switching the initial energy $E_0$ from 20 to 12 keV, corresponding to time $t_s = 25$ s. Here $j_0 = 10^{-3}$ A/m$^2$, $d = 1$ mm, $h = 1$ m.

the second crossover energy $E_{k2}$ in the absence of return of EEE electrons to the emitting surface.

Thus, such an approach makes it possible to simulate the charging of dielectrics upon irradiation with electrons with energies both above and below the second crossover energy $E_{k2}$.

Increasing the current density of the primary beam to 100 nA/cm$^2$ enhances the density of current $j_S(t)$ charging the surface traps (Fig. 14). In this case, the relative fraction of the stored negative charge on the surface of the dielectric in the peak reaches 70% (Fig. 15) of the total stored charge of electrons and holes trapped in deep traps of the bulk.

## 2.3. Discussion of results

The generation of LO-phonon trains, along with the concentration gradient of free deep traps in the near-surface region of the dielectric, leads to the stable negative charging of the dielectric surface. In this case, the fraction of the surface charge can reach about 70% with respect to the total space charge of electrons and holes trapped in deep traps. Although the model can give, in view of the approximations made in the theoretical part, somewhat overestimated results.

The values of the initial energy $E_0(t)$, which are close to the second crossover energy $E_{k2}$, along with the increased current density of the primary beam $j_0$, lead to increase in the fraction of charge trapped on dielectric surface. As a result, strong negative electric fields $F(0, t) \sim 10^7$ V/m are formed, which can shift the second crossover energy to new value $E'_{k2} < E_{k2}$. The developed model is suitable to consider the presence of a plasma environment. In this case, instead of the value of the vacuum gap, one should speak about the Debye length. The decrease in the vacuum gap $h$ leads to a strong increase in the electric field inside the dielectric, which can subsequently lead to electrical breakdown of the dielectric. Such situation can

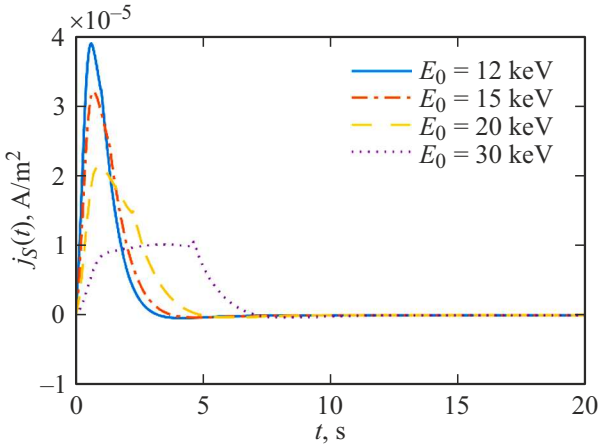


**Figure 14.** Total current density, charging dielectric surface vs. irradiation time at different initial energies of primary electrons $E_0$. Here $j_0 = 10^{-3}$ A/m$^2$, $d = 1$ mm, $h = 1$ m.

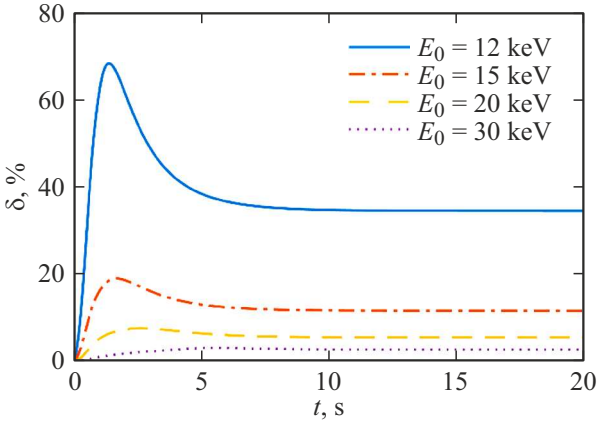


**Figure 15.** Fraction of charge stored on surface traps with relation to total charge in bulk of dielectric at different energies of primary electrons $E_0$. Here $j_0 = 10^{-3}$ A/m$^2$, $d = 1$ mm, $h = 1$ m.

take place when actual dielectrics in geomagnetic plasma are considered, whereas in the case of a random plasma flare in the environment the Debye length can sharply decrease, and the dielectric surface can be charged with positive plasma ions until the surface potential is completely neutralized, $\varphi_S = 0$. The positive charge presence on the surface of the dielectric and small value of $h$ can lead to strong increase in the electric field inside the dielectric to critical values and, as a consequence, breakdown of the dielectric.

In dielectrics of thickness $\sim R_{\max}(E_0)$, the strong outflow of electrons towards the back electrode occurs after quasi-stabilization of the distributions of electrons and holes trapped in deep traps. The largest contribution, along with the dark current, is made by the drift current (enhanced by the Poole-Frenkel effect) in strong electric field. The outflow of electrons into the non-irradiated region of the dielectric leads to shift in the center of mass of the distribution of electrons trapped in deep traps towards the back electrode. The potential of the open surface continues to rise until the distribution of electrons $n_{DT}^{-}(x,t)$ reaches the back electrode, after which the potential rise slows down sharply up to quasi-equilibrium state, while the fly-n energy $E_L(t)$ does not reach second crossover energy $E_{k2}$.

## Conclusion

Thus, using $\alpha$-$Al_2O_3$ as an example, we demonstrated that electron transfer under the action of LO-phonon trains can play a significant role in the presence of concentration gradient of free deep electron traps, as well as strong electric fields, which takes place, in particular, in the near-surface region of actual dielectrics. Accounting for these processes complements the current of „classical“ induced conduction associated with the generation of electron-hole pairs. In particular, the density of acurrent associated with the ionization of deep traps due to LO-phonon trains leads to depletion of the concentration of electrons trapped by deep traps in the near-surface region of strong electric field. The presence of the current density associated with the gradient of free deep traps in the near-surface region in the presence of LO-phonon trains promotes a large outflow of bulk electrons due to tunneling processes through deep traps from the near-surface region to surface traps.

The contribution of currents based on trains to the total induced conductivity increases in proportion to the rise of the primary electron current, which affects the charging of surface deep traps and leads to inversion of the subsurface electric field $\sim -10^5$ V/m. In this case, the fraction of the charge trapped by surface traps reaches $\sim 70\%$ of the total excess charge of the bulk of dielectric for the primary current density 100 nA/cm$^2$.

The model shows that in the simplest case, the total charge distribution of electrons and holes in the bulk of dielectric has the form of „three-mode“ distribution, which differs from representations that take into account distributions corresponding to two modes (two layers): the distribution of holes remaining after the release of SEE electrons; distribution of stopped primary electrons. The presence of such a distribution is due to the consideration of the recombination processes associated with the enhanced ionization of deep traps by means of LO phonons train in regions of strong electric field, as well as the presence of recombination maximum of electrons injected deep into the dielectric with holes left after the generation of electronhole pairs near the second point of zero field $x \approx 10^{-6}$ m.

The switching mode of the primary energy of electrons makes it possible to simulate the charging of the dielectric by electrons with an fly-in energy lower than the second crossover energy $E_{k2} \approx 10$ keV corresponding to the uncharged dielectric $\alpha$-$Al_2O_3$. In mode that does not take into account the switching of the initial energy of electrons, direct simulation with energy below the second crossover energy can lead to difficulties associated with consideration of the part of SEE electrons returned by the electric field.

The decrease in dielectric thickness to values about the maximum range of primary electrons leads to a critical rapid growth of the electric field in the unirradiated part of the dielectric, which can subsequently cause electrical breakdown until the charging mode reaches quasi-equilibrium with respect to the surface potential. In particular, for the dielectric thickness $\sim 100\,\mu$m only currents charging the surface have time to reach quasi-equilibrium.

Accounting for the heterostructure vacuum gap surface bulk of dielectric makes it possible to carry out simulations that include charging the dielectric surface, including by low-energy ions of the vacuum environment (plasma, residual atmosphere).

### Conflict of interest

The authors declare that they have no conflict of interest.

## References

[1] M.I. Panasyuk, L.S. Novikov. *Model kosmosa* (KDU, M., 2007), t. 2, s. 1144. (in Russian)
[2] D.C. Ferguson, R.C. Hoffmann, E.A. Plis, D.P. Engelhart. J. Spacecraft Rockets, **55** (3), 698 (2018). DOI: 10.2514/1.A34017
[3] D.P. Engelhart, E.A. Plis, D. Ferguson, K. Artyushkova, D. Wellems, R. Cooper, R. Hoffmann. IEEE Trans. Plasma Sci., **47** (8), 3848 (2019). DOI: 10.1109/TPS.2019.2921937
[4] D. Ferguson, S. White, R. Rast, E. Holeman. IEEE Trans. Plasma Sci., **47** (8), 3834 (2019). DOI: 10.1109/TPS.2019.2922556
[5] T. Paulmier, D. Lazaro, B. Dirassen, R. Rey, J.-C. Matéo-Velez, D. Payan. IEEE Trans. Plasma Sci., **47** (8), 3776 (2019). DOI: 10.1109/TPS.2019.2922256
[6] D.C. Ferguson, R.C. Hoffmann, D.P. Engelhart, E.A. Plis. IEEE Trans. Plasma Sci., **45** (8), 1972 (2017). DOI: 10.1109/TPS.2017.2694387
[7] D. Ferguson, P. Crabtree, S. White, B. Vayner. J. Spacecraft Rockets, **53** (3), 464 (2016). DOI: 10.2514/1.A33438

[8] K.D. Cummings, M. Kiersh. J. Vac. Sci. Technol. B: Microelectron. Process. Phenom., **7** (6), 1536 (1989). DOI: 10.1116/1.584528
[9] K.T. Arat, T. Klimpel, A.C. Zonnevylle, W.S.M.M. Ketelaars, C.T.H. Heerkens, C.W. Hagen. J. Vac. Sci. Technol. B, **37** (5), 051603 (2019). DOI: 10.1116/1.5120631
[10] S. Fakhfakh, O. Jbara, S. Rondot, A. Hadjadj, J.M. Patat, Z. Fakhfakh. J. Appl. Phys., **108** (9), 093705 (2010). DOI: 10.1063/1.3499692
[11] J. Cazaux. J. Appl. Phys., **59** (5), 1418 (1986). DOI: 10.1063/1.336493
[12] X. Meyza, D. Goeuriot, C. Guerret-Piécourt, D. Tréheux, H.-J. Fitting. J. Appl. Phys., **94** (8), 5384 (2003). DOI: 10.1063/1.1613807
[13] É.I. Rau, E.N. Evstaf'eva, M.V. Andrianov. Phys. Solid State, **50** (4), 621 (2008). DOI:10.1134/S1063783408040057
[14] E.I. Rau, A.A. Tatarintsev. Phys. Solid State, **63** (4), 628 (2021). DOI: 10.1134/S1063783421040181
[15] V.M. Zykov, D.A. Neyman. Russ. Phys. J., **60**, 2201 (2018). DOI: 10.1007/s11182-018-1347-0
[16] H.-J. Fitting, V.S. Kortov, G. Petite. J. Lumin., **122/123**, 542 (2007). DOI: 10.1016/j.jlumin.2006.01.188
[17] K.A. Nasyrov, V.A. Gritsenko. Physics-Uspekhi, **56** (10), 999 (2013). DOI: 10.3367/UFNe.0183.201310h.1099
[18] T. Hosono, K. Kato, A. Morita, H. Okubo. IEEE Trans. Dielectr. Electr. Insul., **14** (3), 627 (2007). DOI: 10.1109/TDEI.2007.369523
[19] G.M. Sessler, M.T. Figueiredo, G.F.L. Ferreira. IEEE Trans. Dielectr. Electr. Insul., **11** (2), 192 (2004). DOI: 10.1109/TDEI.2004.1285887
[20] Yu.N. Novikov, V.A. Gritsenko, K.A. Nasyrov. JETP Lett., **89** (10), 506 (2009). DOI: 10.1134/S0021364009100075
[21] B. Raftari, N.V. Budko, C. Vuik. J. Appl. Phys., **118** (20), 204101 (2015). DOI: 10.1063/1.4936201
[22] M. Belhaj, S. Odof, K. Msellak, O. Jbara. J. Appl. Phys., **88** (5), 2289 (2000). DOI: 10.1063/1.1287131
[23] S.V. Nikiforov. Dokt. diss., Ekaterinburg, Uralsky Federalny universitet imeni pervogo Presidenta Rossii B.N. Eltsin, 2016. (in Russian)
[24] J. Cazaux. Nucl. Instrum. Methods Phys. Res. Sect. B Beam Interact. Mater. At., **244** (2), 307 (2006). DOI: 10.1016/j.nimb.2005.10.006
[25] J.F. Fowler. Proc. R. Soc. London A — Math Phys. Sci., **236** (1207), 464 (1956). DOI: 10.1098/rspa.1956.0149
[26] K.A. Nasyrov, V.A. Gritsenko. J. Exp. Theor. Phys., **112**, 1026 (2011). DOI: 10.1134/S1063776111040200
[27] M.E. Banda, S.L. Roy, V. Griseri, G. Teyssèdre. J. Phys. D: Appl. Phys., **53** (8), 085503 (2019). DOI: 10.1088/1361-6463/ab5692
[28] V.A. Gritsenko, A.A. Gismatulin, A. Chin. Mater. Res. Express, **6** (3), 036304 (2019). DOI: 10.1088/2053-1591/aaf61e
[29] Yu.N. Novikov. Phys. Solid State, **55** (5), 966 (2013). DOI: 10.1134/S1063783413050272
[30] Y.N. Novikov, A.V. Vishnyakov, V.A. Gritsenko, K.A. Nasyrov, H. Wong. Microelectron. Reliab., **50** (2), 207 (2010). DOI: 10.1016/j.microrel.2009.11.004
[31] Yu.N. Novikov, A.V. Vishnyakov, V.A. Gritsenko, K.A. Nasyrov. Izvestiya RGPU im. A.I. Gertsena, (122) 46 (2010) (in Russian).
[32] K.A. Nasyrov, V.A. Gritsenko, Yu.N. Novikov, D.V. Gritsenko, D.-V. Li, Ch.V. Kim. Izvestiya RGPU im. A.I. Gertsena, **5** (13), 147 (2005). (in Russian).
[33] Yu.N. Novikov. Phys. Solid State, **47** (12), 2233 (2005). DOI: 10.1134/1.2142883
[34] K.A. Nasyrov, Yu.N. Novikov, V.A. Gritsenko, S.Y. Yoon, C.W. Kim. JETP Lett., **77**, 385 (2003). DOI: 10.1134/1.1581966
[35] S.D. Ganichev, I.N. Yassievich, W. Prettl. J. Phys.: Condens. Matter., **14** (15), R1263 (2002). DOI: 10.1088/0953- 8984/14/50/201
[36] K.A. Nasyrov, V.A. Gritsenko, M.K. Kim, H.S. Chae, S.D. Chae, W.I. Ryu, J.H. Sok, J.-W. Lee, B.M. Kim. IEEE Electron Device Lett., **23** (6), 336 (2002). DOI: 10.1109/LED.2002.1004227
[37] A.F. Zatsepin, V.G. Mazurenko, V.S. Kortov, V.A. Kalentiev. FTT, **30** (11), 3472 (1988). (in Russian).
[38] V. Karpus, V.I. Perel. J. Exp. Theor. Phys., **91** (6), 2319 (1986).
[39] A. Melchinger, S. Hofmann. J. Appl. Phys., **78** (10), 6224 (1995). DOI: 10.1063/1.360569

*Translated by I.Mazurov*